Yellow-Emitting Hydrophobic Carbon Dots via Solid-Phase Synthesis and Their Applications

Dan Zhao,* Zhixia Zhang, CaiMao Li, Xincai Xiao, Jun Li, Xuemei Liu, and Han Cheng

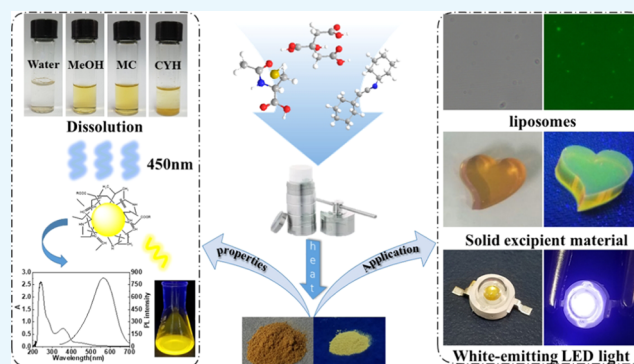Read Online

ACCESS | Metrics & More | Article Recommendations | Supporting Information

ABSTRACT: The preparation and application of hydrophobic carbon dots (HCDs) are now the hotspots in the field of nanomaterials. This paper reports the fast synthesis of long-wavelength-emitting HCDs (yellow-emitting, λ_{em} = 541 nm) through a solid-phase route, with L-cysteine hydrochloride anhydrous and citric acid as carbon sources and dicyclohexylcarbodiimide as a dehydrating agent, reacting at 180 °C for 40 min, with a quantum yield of 30%. The solid-phase route avoids the usage of organic reagents during the synthesis process and is thus environmentally friendly. The obtained HCDs can be simply separated into HCDs-L (less density) and HCDs-W (higher density) with differences in physical (polarity, density), optical, and chemical properties. The differences in HCDs-L, HCDs-W, and water-soluble CDs (WCDs) were compared through various characterization methods, and the synthesis and luminescence mechanisms of HCDs were investigated. Meanwhile, HCDs were employed in the fields of LED lamp production and solid fluorescent shaping material. The prepared HCDs were then modified into WCDs through the liposomal embedding method. The HCDs prepared by the new solid-phase route exhibit stable and highly efficient photoluminescence ability and will have a promising outlook in their applications in various fields.

INTRODUCTION

In recent years, fluorescent nanomaterials have become the focus of researchers because of their excellent optical and chemical properties. Research studies on graphene,[1,2] metal nanoclusters,[3,4] metal quantum dots,[5,6] and carbon dots (CDs) have developed rapidly. As a novel nanomaterial, CDs have acquired a promising outlook in their applications in the fields of sensing,[7,8] biological imaging,[9,10] and drug delivery[11,12] due to their excellent stability and low toxicity. Until now, most prepared CDs are hydrophilic, which would lead to aggregation-caused quenching (ACQ) because of the limitation of surface groups,[13,14] and this would hinder their applications in organic electronics,[15] film application,[16] or detection in the hydrophobic environment.[17] Therefore, hydrophobic CDs (HCDs) have become a new attraction to the researchers.

The synthesis of HCDs is usually classified into two types. The first type modifies prepared water-soluble CDs (WCDs) into hydrophilic ones through surface modification.[18,19] For instance, Shang et al.[18] dissolved the WCDs into toluene and oleylamine with heating (130 °C) and refluxing for 6 h and acquired orange-emitting HCDs with the emission wavelength (λ_{em}) red-shifted by 20 nm. Varisco[19] and his team modified prepared WCDs with ethylenediamine or dodecylamine under heating (115 °C) and stirring for 4 h and acquired HCDs without λ_{em} shifting. This type of synthesis process requires a complicated operation and long reaction time with reduced quantum yields.

Another type of synthesis is a one-step reaction in strong acids,[13,20−22] strong bases,[23] or organic reagents[17,18,24,25] under high temperatures. Usually, ascorbic acid,[26−28] glucose,[17] or octadecylamine[17,24,25,27,28] were used as carbon sources and phosphate,[13,20,21] nitric acid,[22,24] sodium hydroxide,[23] and some organic reagents (toluene[18,24] or 1-octadecene[11,18,19]) as solvents; the reaction temperatures of most of the experiments range from 160 to 280 °C and the reaction times range from 20 min to 12 h.

For instance, Lu et al.[17] acquired blue-emitting HCDs with glucose and octadecylamine as carbon sources (160 °C, 30 min), and Kwon et al.[24] prepared blue-emitting HCDs through adding oleamine and octadecene to the nitric acid solution of citric acid (250 °C, 2 h). Mao et al.[20] mixed ionic liquid BmimPF$_6$ with phosphate (5 mol/L, dissolved in ethanol) for 96 h (200 °C) and centrifuged the mixture to acquire green-

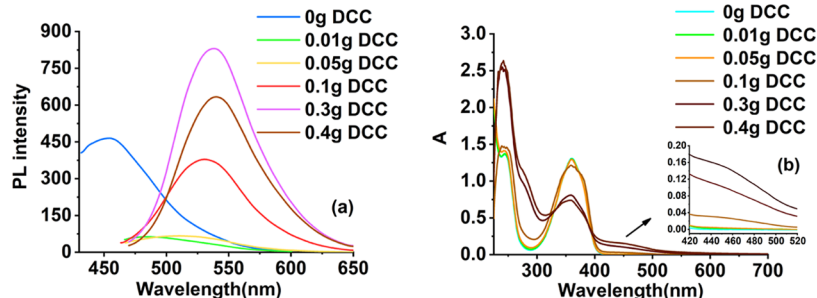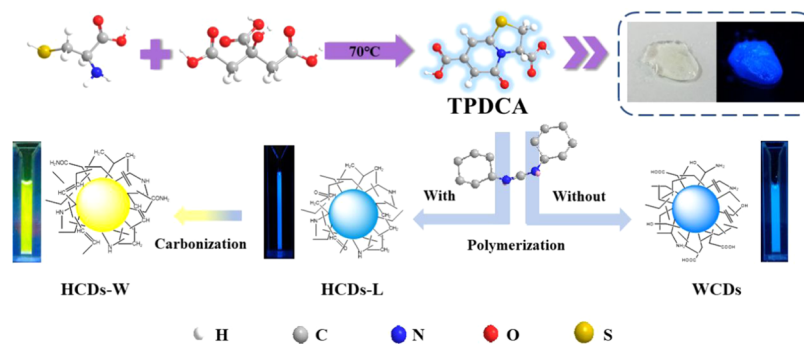**Scheme 1. Proposed Mechanism for HCD Synthesis**

Figure 1. (a) PL spectra of HCDs with different addition masses of oxidant DCC and (b) UV−vis spectra of HCDs with different DCC addition masses (WCDs are dissolved in water, and HCDs are dissolved in dichloromethane).

emitting HCDs. Zheng[23] and his team used hexadecylpyridinium chloride monohydrate and sodium hydroxide as raw materials and acquired green-emitting HCDs after stewing the mixture for 2 h. However, the solvents used in this type of synthesis routes are strong in toxicity and corrosivity, unfriendly to the environment. Meanwhile, since the long-wavelength-emitting HCDs show promising outlook in their applications in optical materials and biological imaging, the development of a simple, fast, and environmentally friendly (avoiding the usage of strong acids, strong bases, and organic reagents) solid-phase synthesis route is the target of this program.

On the other hand, the applications of HCDs are also the focus of the researchers. Thanks to their excellent solid fluorescence properties, HCDs would have promising applications in both liquid and solid phases. In the liquid phase, HCDs can be used in the fields of cell imaging,[29,30] material detection in organic phases,[19,31] the marking of hydrophobic bacteria and antibiosis.[15,16] Cheng et al.[26] applied the prepared green-emitting HCDs for the detection of 2,4,6-trinitrophenol in organic reagents with a detection limit at 1.8 μM. Stanković[16] and his team prepared a hydrophobic film by coating HCDs on different substrates. Based on this film, they realized the antibiosis and antibiotic activity experiments by taking advantage of the properties of HCDs that they release singlet oxygen under irradiation of blue light. Moreover, Talib[29] and his team realized the biological imaging of breast cancer stem cells. Compared with commercial CdSe quantum dots, the imaging effect of HCDs did not show an obvious difference. In its solid phase, the fields like light-emitting diodes (LEDs) and latent fingerprint indication are also a novel platform for the application of HCDs. Jiang[13] and his team applied the prepared white-emitting HCDs to produce a light source of LEDs. Additionally, the −COOH existing on the surface of HCDs would combine with the amino acid on

the surface of latent fingerprint and thus enhance the labeling effect of fingerprint development.

This paper, for the first time, reports a novel, environmentally friendly, and fast solid-phase synthesis method in preparing long-wavelength-emitting HCDs (λ_{em} = 541 nm). With L-cysteine hydrochloride anhydrous (L-cys·HCl) and citric acid monohydrate (CA) as cocarbon sources and dicyclohexylcarbodiimide (DCC) as a dehydrating agent, yellow-emitting HCDs were acquired (180 °C, 40 min) with a quantum yield of 30%. The synthesis and luminescence mechanisms of HCDs, HCDs-L (less density), and HCDs-W (higher density) were explored through multiple characterization methods. Meanwhile, the prepared HCDs have been applied in the production of LED lights and solid fluorescent shaping materials and have been modified into hydrophilic CDs through a liposomal embedding method. This new solid-phase synthesis method avoids the addition of strong acids, strong bases, and organic reagents and thus successfully avoid the environmental pollution during the synthesis. The proposed synthesis mechanism of yellow-emitting HCDs would inspire new synthesis methods for HCDs in the future.

■ RESULTS AND DISCUSSION

Impact of Synthesis Parameters on the Optical Properties of HCDs. Considering the strong corrosivity of strong acids, strong bases, and organic reagents, which do not meet the requirements for green synthesis, a novel solid-phase synthesis route for long-wavelength-emitting HCDs was developed. As shown in Scheme 1, in the first step, the raw materials L-cys·HCL and CA were dissolved in 2 mL of pure water and then heated in an unsealed autoclave (70 °C) for 12 h. A colorless viscous colloid was obtained after all of the water evaporated. The product was speculated as a small-molecular blue-emitting fluorophore 5-oxo-3,5-dihydro-2H-thiazolo[3,2-a]pyridine-3,7-dicarboxylic acid (TPDCA). In the second step,

without the presence of DCC, only water-soluble blue-emitting CDs were acquired. When DCC is added as a dehydrating agent, the small-molecular TPDCA will complete the oxidative dehydration step and yield yellow light-emitting HCD solid powder (Figure S1). What is worth mentioning is that 300 μL of acetonitrile was used as the solvent for DCC to ensure the complete interaction between DCC and the product of the first step. Since the amount of acetonitrile is quite small and it is in a vapor state under high temperatures, this route is still regarded as the solid-state synthesis.

The impacts of synthesis parameters including the ratio of two carbon sources, the amount of DCC, reaction time, and temperature, on the optical properties of prepared HCDs and the possible synthesis mechanism are explored in this part.

The auxiliary material DCC plays a critical role in the synthesis. As shown in Figure 1a, the addition amount of DCC has an obvious impact upon the λ_{em} of prepared HCDs. When the addition amount of DCC increases from 0.0 to 0.1 g, the hydrophilic WCDs become hydrophobic HCDs, and the emission peak red-shifts from 455 to 541 nm. With a further increase of DCC amount to 0.3 g, the extent of red shifting decreases (from 520 to 541 nm). However, the excessive amount of DCC would reduce the fluorescence intensity of prepared HCDs. Figure S2 shows the HCDs prepared by different amounts of DCC. Obviously, with an increase of DCC amount, the prepared HCDs gradually turn from a transparent colorless colloidal solid to a tan dried solid, and the absorption peak at 430 nm also gradually increases (Figure 1b).

Meanwhile, other synthesis parameters were also investigated. Figure 2a−c shows the optical property changes of
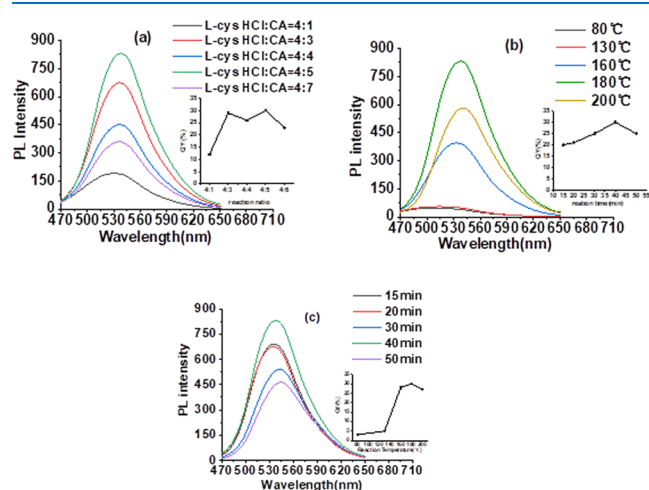

Figure 2. PL spectra of HCDs with different (a) raw material ratios, (b) reaction temperatures, and (c) reaction times (inset: the changes of QYs of HCDs synthesized under different reaction conditions).

prepared HCDs with the adjustments of the ratio of two carbon sources, reaction temperature, and time, respectively. By adjusting the ratio of L-cys·HCl to CA from 4:1 to 4:7, the fluorescence intensity of prepared HCDs reaches maximum at 4:5, which means that this ratio is beneficial to the growth of the carbon core.[32] However, such a ratio change only causes fluorescence intensity change, instead of λ_{em} change. The increases of reaction temperature and time both can lead to the red shift of λ_{em} of prepared HCDs, as shown in Figure 2b,c. Some literature works reported that high reaction temperatures

and long reaction times are beneficial to the dehydration and carbonization processes.[33] Since the synthesis method reported in this paper does not require the dehydration and aggregation processes as a hydrothermal route,[34] longer reaction times and high temperatures also, to some extent, enhance the extent of carbonization of HCDs, reducing its surface defects and then leading to the red shift of the emitting wavelength, which is similar to the effect of DCC in the synthesis process.

Resolving Property of HCDs. We propose that the resolving ability of prepared HCDs is related to the polarity and structure of solvents. Figures 3a and S3 show the results of adding the same amount of HCDs (5 mg) to different solvents. As shown in Figure 3a, HCDs are not soluble in water but soluble in most common organic reagents with polar coefficients between 7.2 and 3.4 (including DMSO, THF, and various alcohols) and slightly soluble in organic reagents with polar coefficients lower than 3.4. Table S1 shows the polar coefficients of various solvents. Meanwhile, it is discovered that HCDs exhibit stronger solubility in certain structured solvents. As shown in Figure 3a, the solubility of HCDs in four solvents with similar polar coefficients differs greatly. They are completely soluble in THF (polar coefficient = 4.2), IPA, and EtOH (polar coefficient = 4.3) but slightly soluble in EA (polar coefficient = 4.3). HCDs are also completely soluble in NBA, whose polar coefficient (3.9) is lower than EA. The good solubility of HCDs in alcohols and THF might be because these solvents are prone to form hydrogen bonds, which could combine with O, N, and H elements on the surface of HCDs, and these van der Waals forces increase the solubility in these solvents. Although the solubility of HCDs is influenced by two factors, the polarity of solvents is still the dominant one. The broad dissolution range of HCDs is beneficial to their further applications in biological imaging and chemical detections.

In the process of understanding the solubility of HCDs, HCDs are also proven to be the mixture with at least two kinds of products with different densities, polarities, and optical properties. As shown in Figure 3a, when using H_2O as a dispersant, there is some powder floating on the upper level of the solution besides the dissoluble powder at the bottom of the solution. In some solvents like Tol, the dissoluble powder only appears at the lower level of the solution, while in CTC, the dissoluble powder all floats on the upper level. Therefore, it can be proposed that HCDs contain at least two different components: one floating on the surface of water and sinking to the bottom of Tol, with intensity at 0.88−1.00 g/cm^3 (Tol-H_2O), which is then labeled as HCDs-L, and another staying at the bottom of water and floating on the surface of CTC, with intensity at 1.00−1.59 g/cm^3 (H_2O−CTC), which is labeled as HCDs-W. This may originate from the structural difference of two HCDs, such as the doping extent of heteroatoms or the tightness extent of the molecular alignment, which will be discussed in detail in the part of the discussion on the synthesis mechanism.

Besides difference in densities, these two powders also show difference in polarities. As shown in Figure 3b, the addition of MeOH into the HCD solution (H_2O/MeOH = 2:1, v/v) would dissolve HCDs-L but not HCDs-W, which means HCDs-L possesses higher polarity than HCDs-W. This might be because HCDs-L have more polar groups on the surface. Moreover, HCDs-L and HCDs-W were separated from the solution through filtration and then dissolved in MeOH and DCM to study their difference in optical properties.
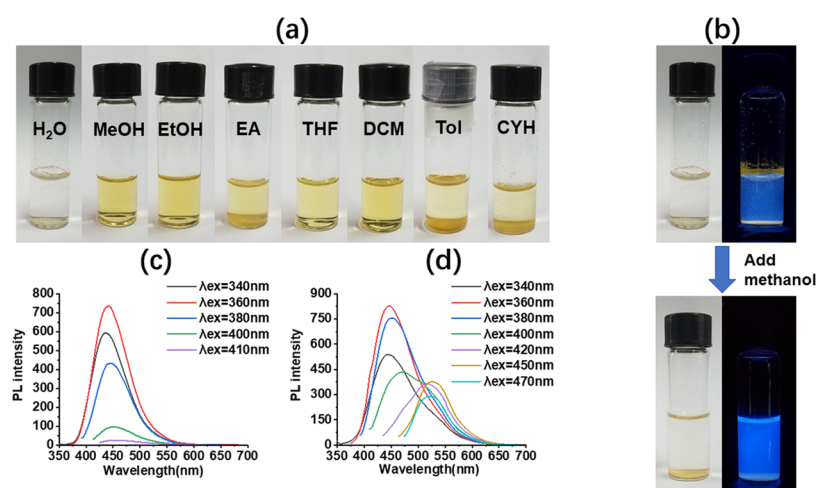
Figure 3. (a) Photos of HCDs dissolved in different solvents, (b) images of HCDs in daylight and ultraviolet light before (up) and after (down) the addition of methanol, and fluorescence spectra of (c) HCDs-L and (d) HCDs-W dissolved in methanol under different excitation wavelengths.
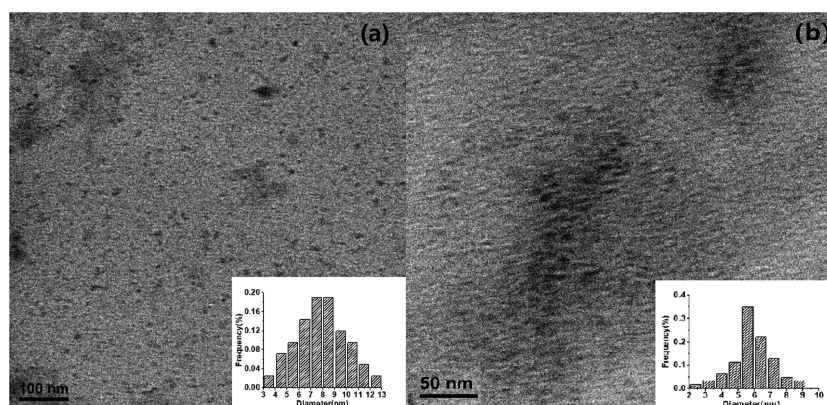

Figure 4. TEM images of (a) WCDs and (b) HCDs and the particle size distributions of WCDs (inset in (a)) and HCDs (inset in (b)).
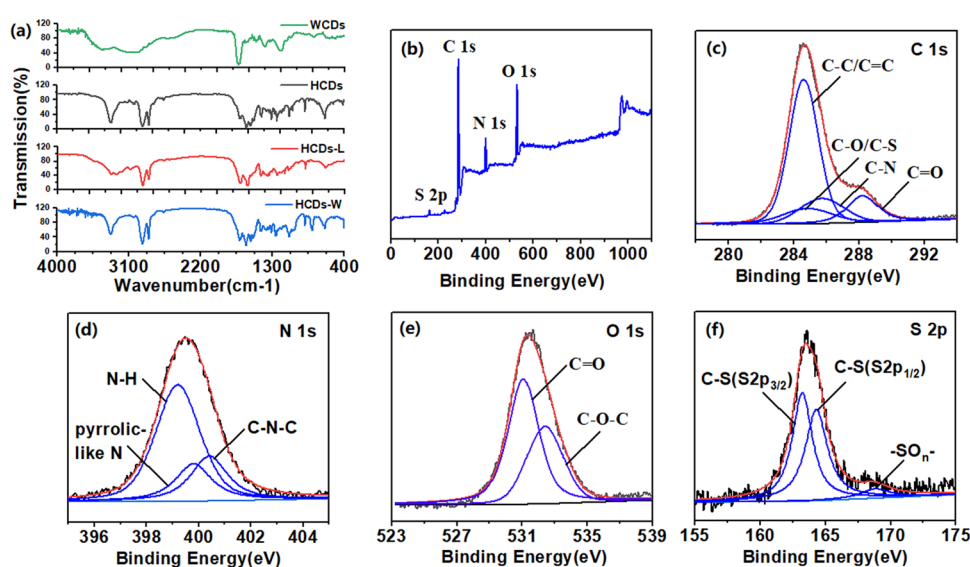

Figure 5. (a) Comparison of IR spectra of four CDs. XPS spectra of HCDs: (b) raw data, (c) C 1s, (d) N 1s, (e) O 1s, and (f) S 2p.

First, the two kinds of HCDs are compared in their illuminating states: HCDs-L are a colorless transparent solution under daylight and emit blue fluorescence under UV light. HCDs-W are a yellow clear and transparent solution and emit green fluorescence under UV light. Their UV−vis spectra are also quite different. At the same mass concentration, HCDs-L had a distinct absorption peak at 352 nm and no significant absorption at 450 nm. HCDs-W had a gentle and broad absorption peak from 352 to 500 nm. Finally, the excitation dependence of HCDs-L and HCDs-W is also

different. With an increase in excitation wavelength (Figure 3c), the λ_{em} of HCDs-L does not show obvious red shifts, which means they do not possess excitation wavelength dependency. Comparatively, HCDs-W show excitation wavelength dependency (Figure 3d). With an increase of excitation wavelength, the emission peak shifts from 450 to 540 nm. The excitation-dependent emission of HCDs-W is due to the rich functional groups on their surface, which can form a series of different fluorophores, thus forming a variety of surface state emission traps.[35,36] Also, we will further characterize HCDs-L and HCDs-W in the following sections to analyze the origins of differences in polarities, densities, and optical properties.

Characterizations of HCDS. To compare the differences in morphologies and crystallinities of WCDs (obtained without DCC during synthesis) and HCDs (obtained by adding DCC), TEM was used to characterize the prepared WCDs and HCDs. As shown in Figure 4, WCDs and HCDs exhibit unique distributions in excellent spherical shape, with the particle diameter of WCDs of about 9.0 nm and HCDs of about 5.8 nm.

The IR spectrum was often used to identify the functional groups on the surface of materials, and was thus used to compare the surface groups on HCDs, HCDs-L, HCDs-W, and WCDs in our research. As shown in Figure 5a, among the IR spectra of the four CDs, the spectra of WCDs show the largest difference. There are hydrophilic groups such as $-NH_2$ (3070 cm^{-1}), $-OH$ (3421, 1397 cm^{-1}), and $-COOH$ (1634 cm^{-1}). These peaks do not appear on the surface of the three HCDs. After adding the dehydrating agent DCC, the hydrophilic groups on the surface of the WCDs are removed to form a hydrophobic structure on the surface. Compared with WCDs, HCDs, and their separated product HCDs-L, IR spectra of HCDs-W are more similar. Both of them show $-NH-$ (3330 cm^{-1}); $-CH_2-$ (2923, 2857 cm^{-1}); $C-S$ (1080 cm^{-1}); and some conjugated groups such as $C=O$ (1704 cm^{-1}), $C=C$ (1026, 639 cm^{-1}), and $C-O-C$ (1241 cm^{-1}). The presence of these hydrophobic bonds also reduces the polarity of the three HCDs. However, there are still some differences in the surfaces of HCDs-L and HCDs-W, such as HCDs-W keep $-NH_2$ (3330, 3247 cm^{-1}) instead of $-NH-$; $CO-NH$ (3300, 1628, 1569 cm^{-1}) not contained in HCDs-L is present in HCDs-W and HCDs. These extra surface groups increase the conjugated system of HCDs and HCDs-W, making their λ_{em} red-shift.

Similar groups can also be observed in the XPS spectrum. Figure 5b shows the four main peaks at 164.1, 284.6, 398.9, and 531.9 eV, attributed to C 1s, N 1s, O 1s, and S 2p, respectively. The C 1s XPS spectra (Figure 5c) proves the existence of $C-C/C=C$ (284.6 eV), $C-N$ (285.4 eV), and $C=O$ (288.2 eV) groups. The XPS spectrum of N 1s (Figure 5d) shows the existence of three fitting peaks, attributed to N–H (399.2 eV), N–C (400.3 eV), and pyrrolic-like N (399.8 eV). The peak at 531.9 eV is attributed to $C=O$ in the O 1s spectrum, and the peak at 532.4 eV is attributed to $C-O-C$ (Figure 5e). The fitting peaks at 163.23, 164.31, and 168.80 eV in the S 2p area spectrum (Figure 5f) show three different components, attributed to $2p_{3/2}$ and $2p_{1/2}$ sites of the $-CS$ covalent bond of thiophene and $-SO_2$, respectively. However, in four-element XPS spectra of WCDs (Figure S4), except for the S 2p fitting peak the same as that of HCDs, the combinations of the rest three elements are different. The spectrum of WCDs shows the existence of $-NH_2$ (401.6 eV) and $-OH$ (532.9 eV) but not $C-N$ (285.4 and 399.58 eV).

The presence of $-OH$ and $-NH_2$ is a source of hydrophilicity for WCDs. Also, the spectra of HCDs-L and HCDs-W (Figure S5) are similar to those of HCDs.

In addition, the C, N, O, and S elements of WCDs, HCDs, HCDs-L, and HCDs-W were used to compare the chemical composition differences. First, comparing WCDs with HCDs, we can find that there are significant differences in their element contents. WCDs contain a large amount of O and C elements but less N and S elements; the contents of N and S elements in HCDs have been greatly improved and that of O element has been decreased. We compared the elemental composition of HCDs-L and HCDs-W and found that the content of S element in HCDs-W is much higher than that of HCDs-L. The large incorporation of S elements with higher relative atomic mass may be responsible for an increase in the density of HCDS-W. When comparing the four sets of data together, we found an interesting phenomenon: The element composition ratio of HCDs-L is closer to that of WCDs and that of HCDs-W is closer to that of HCDs. Their optical properties also show a similar trend (Figure S6): there is no excitation dependence between WCDs and HCDs-L, and their emission wavelengths are around 450 nm (Table 1).

Table 1. Comparison of Element Compositions between HCDS and WCDs

at %	C	N	O	S
WCDs	73.72	2.43	22.57	1.28
HCDs-L	62.43	7.45	27.24	2.89
HCDs-W	47.89	28.91	12.92	10.57
HCDs	53.40	23.72	17.92	4.96

Synthesis and Luminescence Mechanism of HCDs. It is proposed that the hydrophobic and optical properties of HCDs are closely related to their synthesis process. Scheme 1 describes the synthesis process and mechanism with the participation of DCC.

The mixture of carbon sources L-cys·HCl and CA produces a colorless viscous colloid in the first step of synthesis. According to the research of Shi et al.,[32] the colloid is blue-emitting small-molecular TPDCA. Further heating the acquired TPDCA would cause the small molecules in the precursor to experience tangling, aggregation, and carbonization processes to form blue-emitting WCDs. Comparatively, when heating the mixture of TPDCA and DCC, with an increase of DCC amount, the product turns from transparent colloid WCDs into brownish-black solid HCDs. Compared with WCDs, as shown in Figure 2b, the absorption peak of HCDs at 240 nm enhances, illustrating that the $\pi \rightarrow \pi^*$ conjugation enhances in the core of HCDs,[37] and the absorption peak at 360 nm weakens, showing the decreased $n \rightarrow \pi^*$ conjugation on its surface.[38] This phenomenon proves the effect of DCC as a dehydrating agent in the synthesis process, helping the carbonization of the small-molecular polymer, promoting the formation of the carbon core and detaching the hydrophobic groups, such as $-OH$ and $-NH_2$, from the surface of WCDs, which could be proved by the IR and XPS spectra of HCDs and WCDs during the characterization process. The excessive amount of DCC, however, could destroy the fluorophore on the surface of HCDs, decreasing the fluorescence intensity of prepared HCDs.

Because the precursor TPDCA is in a solid state during the reaction, it cannot completely react with DCC uniformly,
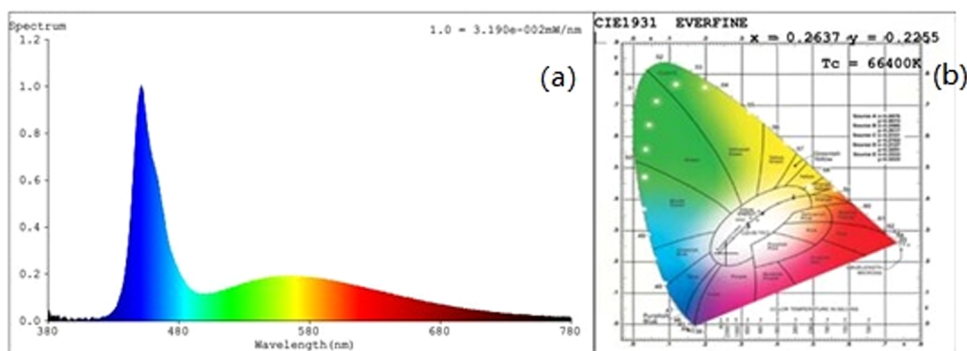
Figure 6. (a) Electroluminescence (EL spectrum) of HCDs and (b) corresponding CIE coordinates of the HCDs.

resulting in HCDs containing various components with different densities, solubilities, and optical properties. This phenomenon was also noticed and reported by some other researchers.[20,39] Mao et al.[20] simultaneously acquired both WCDs and HCDs with ionic liquid BmimNTF$_2$ and phosphate as a carbon source and ethanol as a solvent. Ding[31] and his team used a SiO$_2$ column to separate the one-pot synthesis product prepared by phenylenediamine and urea and acquired eight different emitting CDs.

By comparing the elemental composition and optical properties of WCDs, HCDs, HCDs-L, and HCDs-W, we found that the elemental composition ratios and optical properties of HCDs-L are closer to those of WCDs and those of HCDs-W are closer to those of HCDs. Therefore, we speculate that with the gradual reaction of DCC, WCDs first remove the hydrophilic groups on the surface and become HCDs-L. Then, the diazo bond and the large conjugated structure of DCC are connected to the surface of HCDs-L, so that the content of N element in HCDs-W is further increased, increasing the degree of conjugation of HCDs-W. In this process, L-cys·HCl is also gradually reacted and internalized into HCDs-W to increase its S element doping rate.

Until now, the luminescence mechanism is still controversial. Researchers proposed many models, including a quantum size effect,[40] a luminescence process based on doping of multiple elements,[41] or surface state. In this study, the dehydrating agents work as both the catalyst and reducing agent, directly reacting with hydrophilic luminescent molecule TPDCA. WCDs and HCDs were characterized to study the reason for the red shift of the emission wavelength of HCDs caused by the addition of DCC. As shown in Figure 3a, compared with WCDs, since the λ_{em} of HCDs red-shifts from 452 to 540 nm, together with the smaller particle size of HCDs than that of WCDs shown in TEM (Figure 4), it can be inferred that the red shift of λ_{em} may come from the quantum size effect. As shown in Figure 1, the N content in WCDs (23.72%) is obviously higher than that of HCDs (2.43%). Meanwhile, IR spectra clearly show that the contents of −CH$_2$−, C=O, and CON−H groups on the surface of HCDs are higher than those of WCDs, illustrating that the addition of DCC increases the conjugate system of HCDs, reduces the energy gap, and thus causes the red shift of λ_{em}. Meanwhile, some research studies pointed out that during the separation of the one-step prepared fluorescence-tunable CDs, the enhanced oxidation extent is the main reason for the red shift of λ_{em} of prepared HCDs.[39,42] As a well-known oxidant, DCC plays a critical role in the process of surface modification of HCDs. Therefore, based on the results acquired from experiments and

literature works, we propose that N doping on the surface and the existence of relevant sp^2 groups are critical to the yellow emission of prepared HCDs.

Application of HCDs. The excellent optical properties of the prepared long-wavelength-emitting HCDs and its abilities in dissolving in various solvents promised their applications in various fields, such as in optoelectronic devices[43,44] or *in vivo* or *in vitro* fluorescence imaging probes.[44] The excellent fluorescence of prepared HCDs exhibits its potential application in solid-state lighting and monitoring. Therefore, HCDs were used as a light source in white LED lamps. Figure 6a shows the electroluminescence spectrum of the white LED lamp based on prepared HCDs. The spectrum has two emission bands: blue emission at 450 nm originating from the blue GaN-based chip, and broad yellow emission originating from HCDs. The mixture of two emission bands produces white light. As shown in Figure 6b, the CIE of the produced white LED light is (0.2637, 0.2255), locating in the white light area, which illustrates the successful production of the white LED lamp based on yellow-emitting CDs.

Besides its applications in biological material fields, HCDs also show their potential application as fluorescent solid materials. Addition of a proper amount of HCDs to a mixture of transparent epoxy resin A and epoxy resin B (mass ratio at 3:1) for 24 h under room temperature in a selected mold would produce a solid luminescent shaped material, as shown in Figure 7. This material is hard solid, brown under daylight, and emits yellow fluorescence under irradiation of UV light (365 nm).
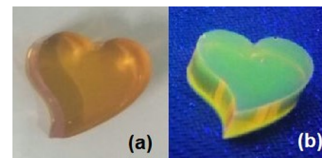

Figure 7. Images of epoxy crafts wrapping CDs under (a) natural light and (b) UV light.

Liposome is a carrier with excellent biological compatibility and is often used to wrap fat-soluble drug molecules or fluorescent nanoparticles for drug delivery[45] and *in vivo* imaging.[46] As shown in Figure 8, since HCDs can insert into the lipid bilayer of liposomes to form liposome−CD (Lipo-CDs) nanostructures, they possess the merits of both: the excellent optical properties of HCDs and the biocompatibility of liposomes. The supporting software of fluorescence microscope MvImage vt 1.0 n was used to measure the
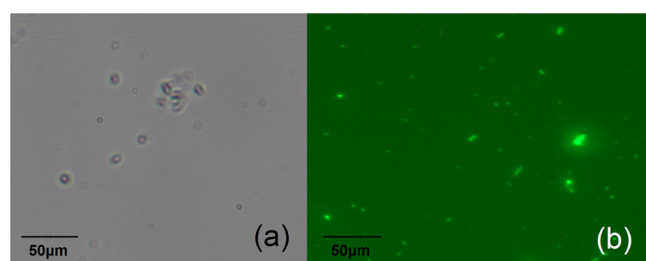
Figure 8. Images of liposomes wrapping CDs under (a) bright field and (b) green light emission.

average particle size of lipo-CD nanostructures, and the average diameter is 400 nm.

The lipo-CD nanostructure exhibits three obvious merits. First, with the wrapping of liposomes, the hydrophobic CDs turns into hydrophilic ones, endowing them biocompatibility for *in vivo* and *in vitro* imaging. Then, the lipid bilayer could prevent the wrapped CDs from escaping from the structure and thus strengthen the wrapping of CDs. Third, considering their applications in target imaging, the surface of lipo-CDs could be further functionalized through attaching of targeting molecules and then ensures their promising outlook in the fields of target imaging and target drug delivery systems.

Compared with some works on hydrophobic CDs published in recent years (Table S2),[13,17,20,23,26,27,47−49] this article provides a new synthetic idea, makes new explorations in the synthesis mechanism, luminescence mechanism, and applications of HCDs, and provides further research on HCDs.

CONCLUSIONS

This paper reports the preparation of yellow-emitting hydrophobic CDs by adding dehydrating agent DCC to the mixture of two carbon sources (L-cys·HCl and CA) for 40 min (180 °C), and the quantum yield of acquired CDs reaches 30% (λ_{em} = 540 nm). The impacts of different synthesis parameters on the optical properties of HCDs were then investigated, and multiple characterization means were used to characterize their optical properties and surface groups for further exploration of the luminescence mechanism of CDs. Meanwhile, the prepared HCDs were wrapped in liposomes to realize the change of hydrophobic CDs to hydrophilic ones. Their applications as solid luminescent shaped materials and the light sources for LED lamps were also explored. The solid-phase synthesis route for preparing HCDs avoids the use of organic reagents and greatly shortens the reaction time to acquire long-wavelength-emitting CDs with high QYs. The highly efficient and stable photoluminescence ability would promise their potential applications in wide range fields as optical materials.

MATERIALS AND METHODS

Reagents and Instruments. L-Cys·HCl (≥99.0%) was obtained from Shanghai Kayon Biological Technology Co., Ltd. DCC (99.0%) and cholesterol (≥95.0%) were purchased from Aladdin Chemistry Co., Ltd. CA (≥99.5%), dimethyl sulfoxide (DMSO, ≥99.0%), methanol (MeOH, ≥99.5%), acetonitrile (CAN, ≥99.0%), acetone (PK, ≥99.0%), ethanol (EtOH, ≥99.7%), ethyl acetate (EA, ≥99.7%), tetrahydrofuran (THF, ≥99.8%), isopropanol (IPA, ≥99.7%), *n*-butyl alcohol (NBA, L ≥99.5%), dichloromethane (DCM, ≥99.5%), toluene (Tol, ≥99.5%), carbon tetrachloride (CTC, ≥99.5%), cyclohexane (CYH, ≥99.5%), potassium dihydrogen phosphate

(≥99.5%), and dipotassium hydrogen phosphate (≥98.0%) were obtained from Sinopharm Chemical Reagent Co., Ltd. Lecithin (BR) were bought from Sinopharm Chemical Reagent Co., Ltd. Blue-emitting LED (Part no. SXS-HP1B0335-460NM) lights were purchased from Shenzhen Sanxin Photoelectric Lighting Technology Co., Ltd. Epoxy resins A and B were bought from Shenzhen Osbang New Material Co., Ltd.

Fluorescence spectra were recorded on a LS55 spectrofluorometer (PerkinElmer). UV−visible absorption spectra were acquired with a Lambda-35 UV−visible spectrophotometer (PerkinElmer) to determine the band gap absorption of HCDs. Fourier transform infrared spectra were obtained on a Nicolet 6700 (IR) spectrometer (Thermo Fisher Scientific), and the sample was tested as a solid powder. Transmission electron microscopy (TEM) images were obtained with a TECNAI G^2 F20 S-TWIN transmission electron microscope (FEI Company). XPS spectra were obtained on a VG Multilab 2000 X-ray photoelectron spectroscope (Thermo Electron Corporation).

All optical measurements were performed at room temperature under ambient conditions. The relative PLQYs of the as-prepared HCDs were measured according to literature works with rhodamine 6G in ethanol (QY = 95%) as a reference standard. All optical measurements were performed at room temperature under ambient conditions.

Synthesis of HCDs. CA (0.5 mmol) and L-cys·HCl (0.4 mmol) were dissolved in 2 mL of water, and the solution was heated in an unsealed Teflon-equipped stainless steel autoclave at 70 °C for 12 h until the products turn into a colorless viscous colloid. The autoclave was heated to 100 °C under the protection of nitrogen gas, and 0.3 g of DCC (dissolved into 300 μL acetonitrile) was then added into the reactor. The mixture was heated under 180 °C for 40 min. Through changing the amount of the raw material, reaction time, and temperature, the impact of synthesis parameters on the properties of the product was explored.

The result product was dissolved in the mixed solution of dichloromethane and methanol (2:1, v/v) and purified through a 1 kD dialysis membrane to obtain HCD powders.

Separation of HCDs. The appropriate amount of water was added to the HCD powder contained in a separate funnel, and the mixture was shaken well and allowed to stand for 30 min. Methanol was added to dissolve HCD-L powder floating on the liquid surface (water/methanol = 2:1, v/v); then, dichloromethane was added to dissolve the HCD-W powder sinking at the bottom of the solution. The HCD-L and HCD-W solutions were poured out separately, and the powder was obtained after drying.

WLED Light. The white-light-emitting device was prepared. For the fabrication of the white-light-emitting device, a blue-emitting chip with the peak wavelength centered at ~460 nm was attached to the bottom of the LED base. The two leads on the battery were prepared to connect to the power supply. Afterward, the epoxy resin was mixed with HCD dissolution (HCDs/resin = 1:10, v/v) and then sonicated to remove the bubbles. The HCDs/resin mixtures were dispensed on the LED chip and thermally cured at 60 °C for 1 h.

Preparation of Solid-Shaped Materials. First, resins A and resin B were mixed uniformly (2:1, m/m); then, the appropriate amount of HCDs was added to the solution. After removing bubbles, the mixed colloid was poured into a mold

and allowed to stand at room temperature. After 24 h, the mold was taken out.

Preparation of Liposomes. Lecithin (25 mg), 10 mg of cholesterol, and an appropriate amount of HCDs were uniformly dispersed in an appropriate amount of the organic reagent. A liposome film was obtained under vacuum distillation under reduced pressure. 20 mM PBS buffer was slowly added into the container, and the solution was ultrasounded for 5 min and then was purified with a 0.22 μm filter. Liposomes encapsulating HCDs were obtained.

ASSOCIATED CONTENT

Supporting Information

The Supporting Information is available free of charge at https://pubs.acs.org/doi/10.1021/acsomega.0c03239.

Images of the acquired HCD powder under daylight and UV light; images of the obtained products with the increase of DCC amount; images of HCDs dissolved in different solvents; polarity coefficients of HCD solvents; XPS spectra of the prepared WCDs; XPS spectra of the prepared HCDs-L and HCDs-W; fluorescence spectra of WCDs and HCDs under different excitation wavelengths; and comparison of this paper and other recently published papers for discussions on synthesis mechanism, luminescence mechanism, and the application of prepared products (PDF)

AUTHOR INFORMATION

Corresponding Author

Dan Zhao — *School of Pharmaceutical Sciences, South-Central University for Nationalities, Wuhan 430074, P. R. China;* orcid.org/0000-0002-9500-7410; Phone: +86-18062084690; Email: wqzhdpai@163.com

Authors

Zhixia Zhang — *School of Pharmaceutical Sciences, South-Central University for Nationalities, Wuhan 430074, P. R. China*

CaiMao Li — *School of Pharmaceutical Sciences, South-Central University for Nationalities, Wuhan 430074, P. R. China*

Xincai Xiao — *School of Pharmaceutical Sciences, South-Central University for Nationalities, Wuhan 430074, P. R. China*

Jun Li — *School of Pharmaceutical Sciences, South-Central University for Nationalities, Wuhan 430074, P. R. China*

Xuemei Liu — *School of Pharmaceutical Sciences, South-Central University for Nationalities, Wuhan 430074, P. R. China*

Han Cheng — *School of Pharmaceutical Sciences, South-Central University for Nationalities, Wuhan 430074, P. R. China*

Complete contact information is available at:
https://pubs.acs.org/10.1021/acsomega.0c03239

Notes

The authors declare no competing financial interest.

ACKNOWLEDGMENTS

REFERENCES

(1) Ulaganathan, R. K.; Chang, Y. H.; Wang, D. Y.; Li, S. S. Light and Matter Interaction in Two-Dimensional Atomically Thin Films. *Bull. Chem. Soc. Jpn.* **2018**, *91*, 761−771.

(2) Shin, B.; Park, J. S.; Chun, H. S.; Yoon, S.; Kim, W. K.; Lee, J. A fluorescence/colorimetric dual-mode sensing strategy for miRNA based on graphene oxide. *Anal. Bioanal. Chem.* **2019**, *412*, 1−10.

(3) Kang, X.; Zhu, M. Tailoring the photoluminescence of atomically precise nanoclusters. *Chem. Soc. Rev.* **2019**, *48*, 2422−2457.

(4) Yu, H. Z.; Rao, B.; Jiang, W.; Yang, S.; Zhu, M. Z. The photoluminescent metal nanoclusters with atomic precision. *Coord. Chem. Rev.* **2019**, *378*, 595−617.

(5) Iida, K.; Uehigashi, Y.; Ichida, H.; Bu, H.-B.; Kim, D. Synthesis of water-soluble $CuInS_2$ quantum dots by a hydrothermal method and their optical properties. *Bull. Chem. Soc. Jpn.* **2019**, *92*, 930−936.

(6) VanWie, T.; Wysocki, E.; McBride, J. R.; Rosenthal, S. J. Bright Cool White Emission from Ultrasmall CdSe Quantum Dots. *Chem. Mater.* **2019**, *31*, 8558−8562.

(7) Yue, J.; Li, L.; Cao, L.; Zan, M. H.; Yang, D.; Wang, Z.; Chang, Z. M.; Mei, Q.; Miao, P.; Dong, W. F. Two-Step Hydrothermal Preparation of Carbon Dots for Calcium Ion Detection. *ACS Appl. Mater. Interfaces* **2019**, *11*, 44566−44572.

(8) Yan, F.; Bai, Z.; Zu, F.; Zhang, Y.; Sun, X.; Ma, T.; Chen, L. Yellow-emissive carbon dots with a large Stokes shift are viable fluorescent probes for detection and cellular imaging of silver ions and glutathione. *Mikrochim. Acta* **2019**, *186*, 113.

(9) Du, J.; Xu, N.; Fan, J.; Sun, W.; Peng, X. Carbon Dots for In Vivo Bioimaging and Theranostics. *Small* **2019**, *15*, No. 1805087.

(10) Shi, C.; Qi, H.; Ma, R.; Sun, Z.; Xiao, L.; Wei, G.; Huang, Z.; Liu, S.; Li, J.; Dong, M.; Fan, J.; Guo, Z. N,S-self-doped carbon quantum dots from fungus fibers for sensing tetracyclines and for bioimaging cancer cells. *Mater. Sci. Eng., C* **2019**, *105*, No. 110132.

(11) Gao, P.; Liu, S.; Su, Y.; Zheng, M.; Xie, Z. Fluorine-Doped Carbon Dots with Intrinsic Nucleus-Targeting Ability for Drug and Dye Delivery. *Bioconjugate Chem.* **2020**, *31*, 1−10.

(12) Das, P.; Ganguly, S.; Agarwal, T.; Maity, P.; Ghosh, S.; Choudhary, S.; Gangopadhyay, S.; Maiti, T. K.; Dhara, S.; Banerjee, S.; Das, N. C. Heteroatom doped blue luminescent carbon dots as a nano-probe for targeted cell labeling and anticancer drug delivery vehicle. *Mater. Chem. Phys.* **2019**, *237*, No. 121860.

(13) Jiang, B. P.; Yu, Y. X.; Guo, X. L.; Ding, Z. Y.; Zhou, B.; Liang, H.; Shen, X. C. White-emitting carbon dots with long alkyl-chain structure: Effective inhibition of aggregation caused quenching effect for label-free imaging of latent fingerprint. *Carbon* **2018**, *128*, 12−20.

(14) Zheng, J. X.; Wang, Y. L.; Zhang, F.; Yang, Y. Z.; Liu, X. G.; Guo, K. P.; Wang, H.; Xu, B. S. Microwave-assisted hydrothermal synthesis of solid-state carbon dots with intensive emission for white light-emitting devices. *J. Mater. Chem. C* **2017**, *5*, 8105−8111.

(15) Gude, V. Synthesis of hydrophobic photoluminescent carbon nanodots by using L-tyrosine and citric acid through a thermal oxidation route. *Beilstein J. Nanotechnol.* **2014**, *5*, 1513−1522.

(16) Stanković, N.; Bodik, M.; Siffalovic, P.; Kotlar, M.; Micusik, M.; Spitalsky, Z.; Danko, M.; Milivojevic, D.; Kleinova, A.; Kubat, P.; et al. Antibacterial and Antibiofouling Properties of Light Triggered Fluorescent Hydrophobic Carbon Quantum Dots Langmuir-Blodgett Thin Films. *ACS Sustainable Chem. Eng.* **2018**, *6*, 4154−4163.

(17) Lu, L. L.; Feng, C. C.; Xu, J.; Wang, F. Y.; Yu, H. J.; Xu, Z. A.; Zhang, W. Hydrophobic-carbon-dot-based dual-emission micelle for ratiometric fluorescence biosensing and imaging of Cu^{2+} in liver cells. *Biosens. Bioelectron.* **2017**, *92*, 101−108.

(18) Shang, W. H.; Ye, M. T.; Cai, T.; Zhao, L. N.; Zhang, Y. X.; Liu, D.; Liu, S. G. Tuning of the hydrophilicity and hydrophobicity of nitrogen doped carbon dots: A facile approach towards high efficient lubricant nanoadditives. *J. Mol. Liq.* **2018**, *266*, 65−74.

(19) Varisco, M.; Zufferey, D.; Ruggi, A.; Zhang, Y. C.; Erni, R.; Mamula, O. Synthesis of hydrophilic and hydrophobic carbon quantum dots from waste of wine fermentation. *R. Soc. Open Sci.* **2017**, *4*, 170900−170911.

(20) Mao, Q. X.; Wang, W. J.; Hai, X.; Shu, Y.; Chen, X. W.; Wang, J. H. The regulation of hydrophilicity and hydrophobicity of carbon dots via a one-pot approach. *J. Mater. Chem. B* **2015**, *3*, 6013−6018.

(21) Mitra, S.; Chandra, S.; Kundu, T.; Banerjee, R.; Pramanik, P.; Goswami, A. Rapid microwave synthesis of fluorescent hydrophobic carbon dots. *RSC Adv.* **2012**, *2*, 12129−12131.

(22) Zhan, J.; Geng, B. J.; Wu, K.; Xu, G.; Wang, L.; Guo, R. Y.; Lei, B.; Zheng, F. F.; Pan, D. Y.; Wu, M. H. A solvent-engineered molecule fusion strategy for rational synthesis of carbon quantum dots with multicolor bandgap fluorescence. *Carbon* **2018**, *130*, 153−163.

(23) Zheng, B. Z.; Liu, T.; Paau, M. C.; Wang, M. N.; Liu, Y.; Liu, L.; Wu, C. F.; Du, J.; Xiao, D.; Choi, M. M. F. One pot selective synthesis of water and organic soluble carbon dots with green fluorescence emission. *RSC Adv.* **2015**, *5*, 11667−11675.

(24) Kwon, W.; Do, S.; Kim, J. H.; Jeong, M. S.; Rhee, S. W. Control of Photoluminescence of Carbon Nanodots via Surface Functionalization using Para-substituted Anilines. *Sci. Rep.* **2015**, *5*, No. 12604.

(25) Bhunia, S. K.; Saha, A.; Maity, A. R.; Ray, S. C.; Jana, N. R. Carbon Nanoparticle-based Fluorescent Bioimaging Probes. *Sci. Rep.* **2013**, *3*, No. 1473.

(26) Cheng, F. L.; An, X. Q.; Zheng, C.; Cao, S. S. Green synthesis of fluorescent hydrophobic carbon quantum dots and their use for 2,4,6-trinitrophenol detection. *RSC Adv.* **2015**, *5*, 93360−93363.

(27) Galyean, A. A.; Behr, M. R.; Cash, K. J. Ionophore-based optical nanosensors incorporating hydrophobic carbon dots and a pH-sensitive quencher dye for sodium detection. *Analyst* **2018**, *143*, 458−465.

(28) Ali, H.; Bhunia, S. K.; Dalal, C.; Jana, N. R. Red Fluorescent Carbon Nanoparticle-Based Cell Imaging Probe. *ACS Appl. Mater. Interfaces* **2016**, *8*, 9305−9313.

(29) Talib, A.; Pandey, S.; Thakur, M.; Wu, H. F. Synthesis of highly fluorescent hydrophobic carbon dots by hot injection method using Paraplast as precursor. *Mater. Sci. Eng., C* **2015**, *48*, 700−703.

(30) Shu, Y.; Lu, J.; Mao, Q. X.; Song, R. S.; Wang, X. Y.; Chen, X. W.; Wang, J. H. Ionic liquid mediated organophilic carbon dots for drug delivery and bioimaging. *Carbon* **2017**, *114*, 324−333.

(31) Ganiga, M.; Mani, N. P.; Cyriac, J. Synthesis of Organophilic Carbon Dots, Selective Screening of Trinitrophenol and a Comprehensive Understanding of Luminescence Quenching Mechanism. *ChemistrySelect* **2018**, *3*, 4663−4668.

(32) Shi, L.; Yang, J. H.; Zeng, H. B.; Chen, Y. M.; Yang, S. C.; Wu, C.; Zeng, H.; Yoshihito, O.; Zhang, Q. Q. Carbon dots with high fluorescence quantum yield: the fluorescence originates from organic fluorophores. *Nanoscale* **2016**, *8*, 14374−14378.

(33) Han, B. Y.; Li, Y.; Peng, T. T.; Yu, M. B.; Hu, X. X.; He, G. H. Fluorescent carbon dots directly derived from polyethyleneimine and their application for the detection of Co^{2+}. *Anal. Methods* **2018**, *10*, 2989−2993.

(34) De, B.; Karak, N. A green and facile approach for the synthesis of water soluble fluorescent carbon dots from banana juice. *RSC Adv.* **2013**, *3*, 8286−8290.

(35) Zhu, S. J.; Song, Y. B.; Zhao, X. H.; Shao, J. R.; Zhang, J. H.; Yang, B. The photoluminescence mechanism in carbon dots (graphene quantum dots, carbon nanodots, and polymer dots): current state and future perspective. *Nano Res.* **2015**, *8*, 355−381.

(36) Barati, A.; Shamsipur, M.; Abdollahi, H. Carbon dots with strong excitation-dependent fluorescence changes towards pH. Application as nanosensors for a broad range of pH. *Anal. Chim. Acta* **2016**, *931*, 25−33.

(37) Hamd-Ghadareh, S.; Salimi, A.; Parsa, S.; Fathi, F. Simultaneous biosensing of CA125 and CA15-3 tumor markers and imaging of OVCAR-3 and MCF-7 cells lines via bi-color FRET phenomenon using dual blue-green luminescent carbon dots with single excitation wavelength. *Int. J. Biol. Macromol.* **2018**, *118*, 617−628.

(38) Xie, H. Z.; Dong, J.; Duan, J. L.; Waterhouse, G. I. N.; Hou, J. Y.; Ai, S. Y. Visual and ratiometric fluorescence detection of Hg^{2+} based on a dual-emission carbon dots-gold nanoclusters nanohybrid. *Sens. Actuators, B* **2018**, *259*, 1082−1089.

(39) Ding, H.; Yu, S. B.; Wei, J. S.; Xiong, H. M. Full-Color Light-Emitting Carbon Dots with a Surface-State-Controlled Luminescence Mechanism. *ACS Nano* **2016**, *10*, 484−491.

(40) Eda, G.; Lin, Y. Y.; Mattevi, C.; Yamaguchi, H.; Chen, H. A.; Chen, I. S.; Chen, C. W.; Chhowalla, M. Blue Photoluminescence from Chemically Derived Graphene Oxide. *Adv. Mater.* **2010**, *22*, 505−509.

(41) Peng, H.; Li, Y.; Jiang, C. L.; Luo, C. H.; Qi, R. J.; Huang, R.; Duan, C. G.; Travas-Sejdic, J. Tuning the properties of luminescent nitrogen-doped carbon dots by reaction precursors. *Carbon* **2016**, *100*, 386−394.

(42) Bao, L.; Liu, C.; Zhang, Z. L.; Pang, D. W. Photoluminescence-Tunable Carbon Nanodots: Surface-State Energy-Gap Tuning. *Adv. Mater.* **2015**, *27*, 1663−1668.

(43) Chen, T. S.; Zhang, Q. X.; Xie, Z. J.; Tan, C. W.; Chen, P.; Zeng, Y. Q.; Wang, F. L.; Liu, H. J.; Liu, Y.; Liu, G. G.; Lv, W. Y. Carbon nitride modified hexagonal boron nitride interface as highly efficient blue LED light-driven photocatalyst. *Appl. Catal., B* **2018**, *238*, 410−421.

(44) Khan, W. U.; Wang, D. Y.; Wang, Y. H. Highly Green Emissive Nitrogen-Doped Carbon Dots with Excellent Thermal Stability for Bioimaging and Solid-State LED. *Inorg. Chem.* **2018**, *57*, 15229−15239.

(45) Franzé, S.; Marengo, A.; Stella, B.; Minghetti, P.; Arpicco, S.; Cilurzo, F. Hyaluronan-decorated liposomes as drug delivery systems for cutaneous administration. *Int. J. Pharm.* **2018**, *535*, 333−339.

(46) Wieland, K.; Ramer, G.; Weiss, V. U.; Allmaier, G.; Lendl, B.; Centrone, A. Nanoscale chemical imaging of individual chemo-therapeutic cytarabine-loaded liposomal nanocarriers. *Nano Res.* **2019**, *12*, 197−203.

(47) Li, J. F.; Li, P. X.; Wang, D. X.; Dong, C. One-pot synthesis of aqueous soluble and organic soluble carbon dots and their multi-functional applications. *Talanta* **2019**, *202*, 375−383.

(48) Yang, H. Y.; Liu, Y. L.; Guo, Z. Y.; Lei, B. F.; Zhuang, J. L.; Zhang, X. J.; Liu, Z. M.; Hu, C. F. Hydrophobic carbon dots with blue dispersed emission and red aggregation-induced emission. *Nat. Commun.* **2019**, *10*, No. 1789.

(49) Gao, W.; Zhou, Y.; Xu, C.; Guo, M.; Qi, Z.; Peng, X.; Gao, B. Bright hydrophilic and organophilic fluorescence carbon dots: One-pot fabrication and multi-functional applications at visualized Au^{3+} detection in cell and white light-emitting devices. *Sens. Actuators, B* **2019**, *281*, 905−911.